Photocatalysis for continuous air purification in wastewater treatment plants: from lab to reality

R. Portela[a,b*], R.F.Tessinari[a,c], S. Suárez[a], S.B. Rasmussen[b], M.D. Hernández-Alonso[a], M.C. Canela[c], P. Ávila[b], B. Sánchez[a*]

[a] CIEMAT-PSA-Environmental Applications of Solar Radiation. Madrid, Spain.

[b] ICP-CSIC. Cantoblanco, Madrid, Spain.

[c] UENF-CCT-Chemical Sciences Lab. Campos dos Goytacazes-RJ, Brazil.

contact e-mail: benigno.sanchez@ciemat.es, raquel.portela@csic.es

TABLE OF CONTENTS

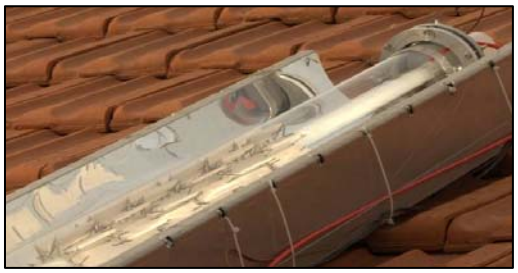

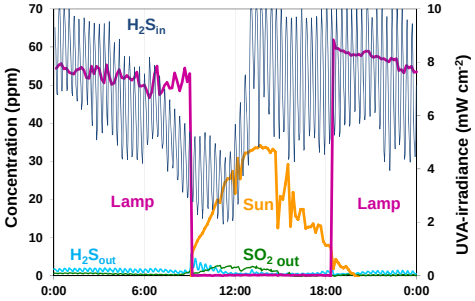

ABSTRACT

The photocatalytic efficiency of TiO_2-$SiMgO_x$ plates to oxidise H_2S was first evaluated in a flat laboratory reactor with 50 ml min^{-1} synthetic air containing 100 ppm H_2S in the presence of humidity. The use of the photocatalyst-adsorbent hybrid material enhanced the photocatalytic activity in terms of pollutant conversion, selectivity and catalyst lifetime compared to previous H_2S tests with pure TiO_2, since total H_2S elimination was maintained for more than 30 operating hours with SO_2 appearing in the outlet as reaction product only after 18 h. Subsequently, the hybrid material was successfully tested in a photoreactor prototype to treat real polluted air in a wastewater treatment plant. For this purpose, a new tubular photocatalytic reactor that may use solar radiation in combination with artificial radiation was designed; the lamp was turned on when solar UV-A irradiance was below 20 W m^{-2}, which was observed to be the minimum value to assure 100% conversion. The efficient distribution of the opaque photocatalyst inside the tubular reactor was achieved by using especially designed star-shaped structures. These structures were employed for the arrangement of groups of eight TiO_2-$SiMgO_x$ plates in easy-to-handle channelled units, obtaining an adequate flow regime without shading. The prototype continuously removed during one month and under real conditions the H_2S contained in a 1 L min^{-1} air current with a variable inlet concentration in the range of tens of ppmv without release of SO_2.

1 INTRODUCTION

Numerous studies concerning gas phase photocatalytic oxidation (PCO) at laboratory-scale can be found in the literature, see e.g. ref. 1 and 2 and references therein.[1, 2] Nevertheless, there are few studies dealing with air treatment applications at pilot scale, in real conditions,[3, 4] or using solar radiation.[5-7] One reason may be that the photocatalyst characteristics, the irradiation and the fluid dynamics strongly condition the photoreactor design and performance; for example, the advantages of working with fixed bed reactors in usual gas phase applications do not apply to photocatalytic systems. Nowadays monolithic catalysts are used for many non-photocatalytic environmental applications. The large exposed geometric area obtained and the low pressure drop of monolithic structures have made them attractive for heterogeneous catalysis.[8] Moreover, the support may beneficially participate in the catalytic process, e.g. when monoliths are made of porous ceramics[9, 10] or activated carbon,[11] which present adsorption properties.[12, 13] However, these monoliths are opaque and the penetration of light inside the channels is restricted.[14] For photocatalytic applications, modular configurations consisting of shallow monoliths, irradiated by groups of lamps located between them[15] or internally illuminated by optic fibres,[16] are required. These configurations make it complicated the use of tubular reactors, which in the case of fluidized bed reactors facilitate the irradiation of the whole reaction medium and the operation at adequate flow regimes, resulting in greater quantum yields.

In addition to the aforementioned restriction, the application of PCO to remove gaseous pollutants may be limited under certain conditions, such as high humidity or extremely low or high reactant concentrations. Formation of undesired products or deactivation of the photocatalyst can be observed as well.[17] In these situations, the coupling of photocatalysis and adsorption might be of interest. The coupling of both technologies can be performed in a tandem arrangement, either installing an adsorption unit as pre-concentration step,[18] or using the adsorption as backup system,[19] where the adsorbent retains unreacted compounds or by-products. Alternatively, the coupling may be obtained in one single step by means of hybrid materials, such as TiO_2-coated or TiO_2-incorporated adsorbents, where the adsorption capacity enhances the photocatalytic activity and, simultaneously, a photocatalytic regeneration of the adsorbent may take place.

Malodours and corrosive compounds produced during wastewater treatment processes, which may cause high maintenance costs and annoyance to nearby residents if they are not controlled or eliminated, are interesting pollutants for the application of hybrid materials.[20] Most of these compounds are inorganic and organic sulphur molecules produced during the organic material degradation. Some research has been devoted to reduce their concentration by heterogeneous photocatalysis;[21-24] however, the deactivation of the photocatalyst and the production of SO_2 as by-product are inconveniences which must be addressed.[24, 25] In precedent works, hybrid materials containing photocatalytically active TiO_2, and sepiolite ($SiMgO_x$) as adsorbent and support, showed excellent performance for the elimination of trichloroethylene in gas phase; the characteristic distribution of the TiO_2 and the sepiolite fibres positively enhanced the selectivity to CO_2. [26-28] The advantage of employing these hybrid materials to both avoid SO_2 release during H_2S photocatalytic oxidation and enhance $SiMgO_x$ capacity for H_2S adsorption was envisaged in previous works, where TiO_2-$SiMgO_x$ coated glass plates were employed.[29, 30] Since the coating resistance of these photocatalysts is not enough for field tests, in this study extruded TiO_2-$SiMgO_x$ plates are employed instead.

The final purpose of this work is achieving the continuous photocatalytic purification of real air, contaminated with H_2S and other volatile organic compounds, at wastewater treatment plants. With this aim, the photocatalytic/adsorbent material is first tested at lab scale and then at a wastewater treatment plant. For the field tests, a novel photoreactor prototype is used, where, for the first time, solar and artificial radiation are employed in a complementary mode.

2 EXPERIMENTAL

The preparation of the incorporated TiO_2-$SiMgO_x$ plates calcined at 500ºC was previously detailed.[26]

The experimental set-up for the laboratory tests, where a flat reactor and UV-A irradiation were used and H_2S and SO_2 concentrations were measured with a Varian CP4900 micro-GC equipped with a m-TCD, is well described elsewhere;[30] the piping and instrumentation diagram is included in the supporting information (Figure S1).

For the field tests, the plates were distributed inside a tubular reactor with the help of star-shaped structures. The experimental set-up installed at the WWTP is shown in Figure 1.

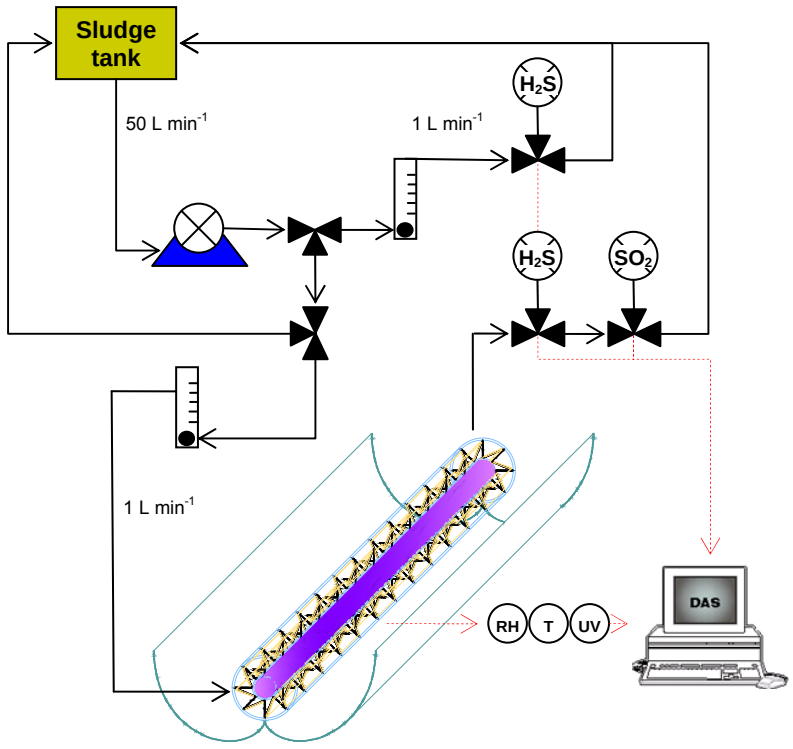

Figure 1. Piping and instrumentation diagram of the photocatalytic experimental set-up at the WWTP.

The annular photoreactor employed comprises two concentric borosilicate glass tubes (D_{ext} = 84mm, D_{int} = 32mm)., The space in-between was filled with channeled photocatalytic units, each of them composed by eight plate-shaped opaque TiO_2-$SiMgO_x$ pieces. The eight plates were fixed by two hollow structures in the form of a star-shaped concave polygon with 8-fold rotational symmetry.[31] The sun was employed as external radiation source, complemented by an internal artificial radiation source (CLEO Effect 70W SLV, λ_{max}= 350 nm, Philips) with the aim

of maximizing the irradiated catalytic surface and enabling nightime operation; the radiation was reflected by a non-concentrating Compound Parabolic Collector (CPC). An automated system was adjusted to switch the lamp on and off depending on the incident solar radiation. A type K- thermocouple and a calibrated UV-radiation sensor (G5842, Hamamatsu) were placed on the CPC aperture plane to measure the ambient temperature and the incident solar irradiance. An additional UV sensor was fixed on the lamp in order to measure the lamp irradiance. The reactor was fed with 1 L min^{-1} air taken from the primary sludge sieve. H_2S and SO_2 were monitored on-line with electrochemical sensors (Zareba Sensepoint, Honeywell Analytics, 0-50 ppmv) placed in the reactor inlet and outlet.

Thermal Gravimetric Mass Spectrometry (TG-MS) analysis was carried out using a Seiko SSC 5200 TG-DTA 320 system coupled to a ThermoStar Balzers Instrument. The samples, of about 20 mg, were treated at room temperature for 20 min under a 500 mL min^{-1} helium flow. Then, the flow was diminished to 100 mL min^{-1} and the system was heated to 1000 °C, with a heating rate of 5°C min^{-1}.

The DRIFTS studies of the hybrid material under study were carried out in a Thermo Nicolet 5700 spectrometer equipped with a liquid N_2-cooled MCT detector and a Praying Mantis device (Harrick). The spectra were registered after accumulation of 64 scans at a resolution of 4 cm^{-1}.

XPS analysis was performed with a Perkin-Elmer PHI 5400 spectrometer equipped with a Mg Kα excitation source ($h\nu$=1253.6 eV) and a beam size of 1 mm diameter. Typical operation conditions were: x-ray gun, 15 kV, 20 mA; pressure in the sample chamber ~ 10^{-9} Torr; pass energy, 44.75 eV for general spectra (0-1100 eV) and 17.5 eV for high resolution spectra. In order to take into account the charging effects on the measured binding energies, these energies have been determined by referencing to the adventitious C 1s peak at 284.6 eV.

The total specific surface areas, S_{BET}, were obtained from the corresponding nitrogen adsorption isotherms at −196°C using a Thermo Electron Corporation Sorptomatic 1990 apparatus, after application of the BET equation in the relative pressure range 0.05–0.35 p/p°. Prior to N_2 adsorption the samples were outgassed overnight at 150°C to a vacuum of $<10^{-4}$ Pa to ensure a dry clean surface, free from any loosely held adsorbed species. The external surface areas were determined with the Harkins-Jura t-Plot. The porosity studies were completed by mercury intrusion porosimetry (MIP) using a CE Instruments Pascal 140/240 and applying the Washburn equation for cylindrical pores, with the values recommended by the IUPAC of 141° and 484 mN m^{-1}, respectively for the contact angle and surface tension of mercury.

3 RESULTS AND DISCUSSION

In preliminary studies, glass plates coated with TiO_2 and TiO_2-$SiMgO_x$ powder were photocatalytically tested and promising results were obtained.[30] Despite the especially good performance of the photocatalyst containing $SiMgO_x$, the poor adherence of the coating on glass poses a practical problem for the application of these photocatalysts. Alternatively, TiO_2-$SiMgO_x$ ceramic plates can be directly obtained by extrusion of the mixture with water, avoiding the use of any inert support and the coating process; therefore incorporated TiO_2-$SiMgO_x$ plates calcined at 500ºC were selected for this study. The characterization of this material can be found elsewhere.[26] The pore size distribution of the freshly calcined sample can be found in the supplementary Figure S2. It exhibits macropores with a pore diameter in the vicinity of the 100 nm, originating from inter TiO_2 particular void space, partly filled with the $SiMgO_X$ matrix, an effect also observed for sulfated zirconia-$SiMgO_x$ matrices.[32] Furthermore, there are channel-like mesopores from the bundled sepiolitic fibers in the pore diameter range of 20 to 50 nm and

other type of smaller mesopores from the roughness of the TiO_2 particles of around 5-8 nm. Finally, there is an almost negligible contribution from micropores, responsible for only 5 $m^2\ g^{-1}$ of the total S_{BET}.

3.1 H_2S and SO_2 photocatalytic degradation on incorporated TiO_2-$SiMgO_x$ plates at laboratory scale.

The photocatalytic activity of the plates was first tested in a laboratory flat reactor, to confirm the good results obtained with the coated glass.[29, 30] Two similar tests were performed with fresh TiO_2-$SiMgO_x$ photocatalytic plates that treated a gas stream of 50 ml min^{-1} containing 1.3% $H_2O_{(g)}$ (30%RH at 30 ºC). In one of the tests H_2S was the target pollutant, while in the other experiment SO_2 was the treated compound, since it is a gaseous by-product in the H_2S photocatalytic oxidation reaction. The inlet concentration was 100 ppmv in both tests. Figure 2 displays the evolution of H_2S or SO_2 concentrations, as well as the accumulated amount of pollutant removed from the gas stream per mass of catalyst over time.

After stabilization of the pollutant and water vapor concentration values in by-pass, the gas stream was passed through the irradiated photoreactor, initially covered by a UV filter in order to observe the adsorption behavior of the sample. The SO_2 adsorption was complete during the first 10 hours, while the H_2S adsorption accounted for only the 60% of the inlet concentration and was not maintained over time, as a result of the lower H_2S sorption kinetics and the poor dynamic H_2S adsorption capacity of the material in these conditions. The active sites were gradually saturated until a dynamic equilibrium was reached, at around 10% adsorption for both pollutants. This happened after 90h for SO_2 and after 20h for H_2S. At this point, the UV filter was removed to study the photocatalytic reaction.

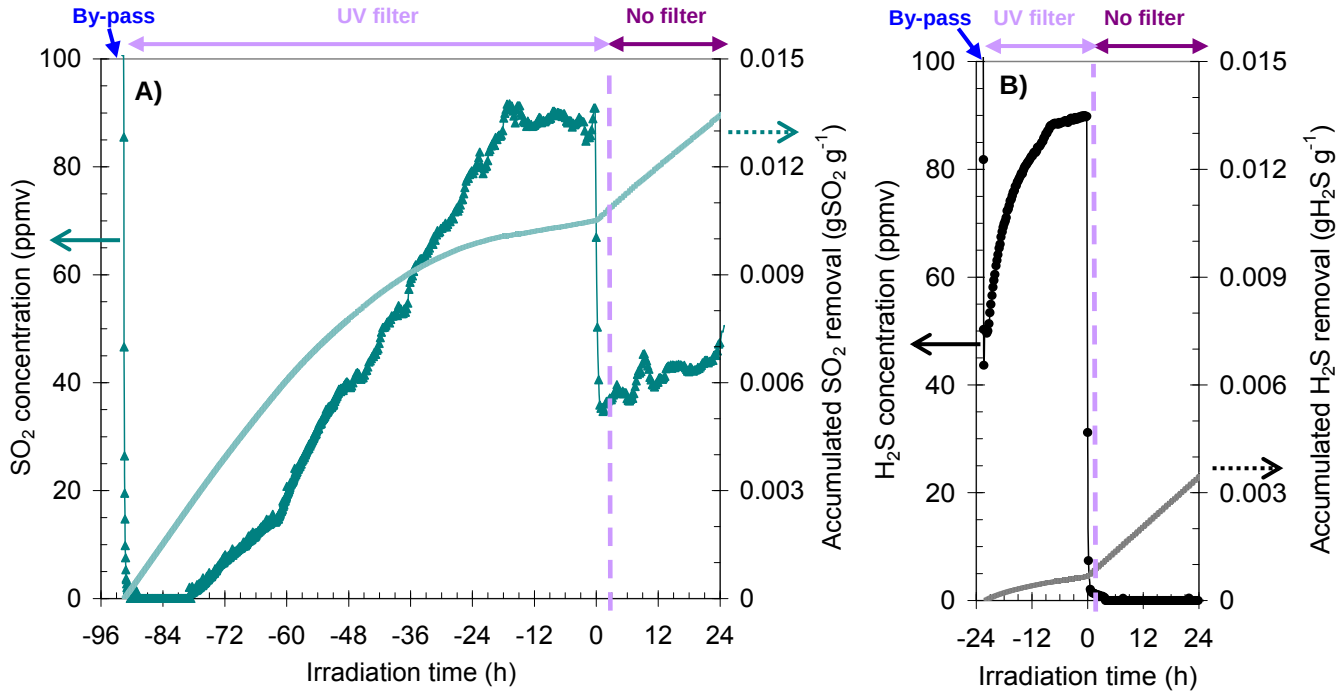

Figure 2. Comparative irradiation tests with a continuous flow of 50 ml min^{-1} containing 1.3% H_2O_v and 100 ppmv of SO_2 (left, ▲) or H_2S (right, ●). Negative times correspond to the dynamic pre-adsorption step (UV filter), and positive times to the subsequent photocatalytic step.

Under irradiation, 100% H_2S conversion was achieved and maintained for more than 30h, with SO_2 appearing in the outlet as reaction product after 18h of H_2S photocatalytic degradation (not shown in the graph for clarity reasons), which is an evident advance in terms of lifetime with respect to the results obtained with pure TiO_2, where SO_2 appeared during the first hour.[33] The positive effect of employing sepiolite as TiO_2 support could be related not only to the increased adsorption capacity of both the pollutant and the by-product, but also to the modification of the surface interactions, as observed in the degradation of trichloroethylene.[26] The mechanism of H_2S photocatalytic degradation on TiO_2 proposed in previous works of the authors suggests the formation of SO_2 and SO_4^{2-} as reaction products.[30] Although the role of sepiolite in the photocatalytic process has not been elucidated, there is no evidence that the sepiolite alters the reaction pathway. By XPS analysis only sulfate, and no elemental sulfur, has been identified on the surface and in the gas phase no other sulfur-containing compounds have been detected. Therefore, it seems that the SO_2 is able now to undergo the oxidation to sulfate before its desorption during a much longer irradiation time due to the higher amount or the presence of new type of adsorption sites, which makes the material not so easily saturated. In fact, sepiolite is characterized by a high amount of surface hydroxyls,[34] where SO_2 can be adsorbed.[35]

Only 65% conversion was attained when SO_2 was administered. This result is in agreement to previous photocatalytic tests performed with TiO_2-coated glass plates, with very low adsorption capacity, where it was found that the SO_2 conversion was significantly lower compared to that of H_2S.[33] Additionally, the deactivation is faster in the test with SO_2, even though the initial degree of pre-saturation of the TiO_2-$SiMgO_x$ samples was similar. This effect is opposite to what was observed during the (non-radiated) pre-saturation step. It therefore appears that, despite immediate larger sorption capacity of SO_2 compared to H_2S, the photocatalytic reaction rate seems both relatively slower and more prone to deactivation. The high amounts of SO_x accumulated on the active sites inside the pores compete with the inlet SO_2 during the photocatalytic oxidation.

This hypothesis is supported by the data from N_2 adsorption and Hg intrusion porosimetry in Table 1, where it can be seen that the sample used with SO_2 lost around 25 m^2/g of external surface area. In the H_2S treated sample it can be observed that there is absolutely no change in morphology during the non-photocatalytic pre-saturation step (H_2S_{ads}) because there is no catalytic effect without irradiation, and therefore the material retains only little H_2S. However, after the filter is removed, the H_2S is oxidized facilitating sorption, which influences the morphology of the catalyst, whose external surface decreases (H_2S_{phot}) in a similar manner to that observed for the SO_2 exposed sample. Parallel to this, the area from micropores consistently increases. Though the changes in the pore volumes are not significant and the micropore volumes observed are almost zero cm^3/g, the modifications might be related to e.g. crystalline sulfate formation in smaller mesopores leading to a decrease in mesoporosity and a small increase in microporosity.

Table 1. Pore volume and surface area of the TiO_2-$SiMgO_x$ samples

Surface area ($m^2\ g^{-1}$)			Pore volume ($cm^3\ g^{-1}$)		
External	Micropores	S_{BET}	Micropores	Mesopores	Macropores

Fresh	126	4	130	0.002	0.34	0.25
H_2S_{ads}	126	4	130	0.000	0.35	0.27
H_2S_{phot}	110	8	119	0.003	0.37	0.27
$SO_{2\ phot}$	100	11	111	0.005	0.32	0.23
WWTP	104	9	113	0.004	0.32	0.26

3.2 Semi-pilot plant tests at a Wastewater Treatment Plant (WWTP)

Due to the good photocatalytic activity observed in the flat reactor with TiO_2-$SiMgO_x$ ceramic plates for the elimination of H_2S, an experimental set-up was developed in order to perform experiments with H_2S-polluted real air from a WWTP. With this aim, a new photocatalytic system was designed to allow the adequate distribution of the opaque plates inside an irradiated annular reactor. Photocatalytic units composed by eight TiO_2-$SiMgO_x$ plates were mounted and placed in the space between the reactor concentric tubular walls. A first experiment was performed placing the reactor with three photocatalytic units in the primary sludge management unit and using the internal UV-lamp; subsequently, a second experiment was performed with six photocatalytic units using both the lamp and the sun as complementary radiation sources. With this purpose, the reactor was fixed on the tilted roof of the primary sludge management unit (20º) facing SSE, as shown in Figure 3. It must be pointed out that in both experiments the reactor was only partially filled, so that the days of operation needed before the first signs of deactivation occurred were reduced.

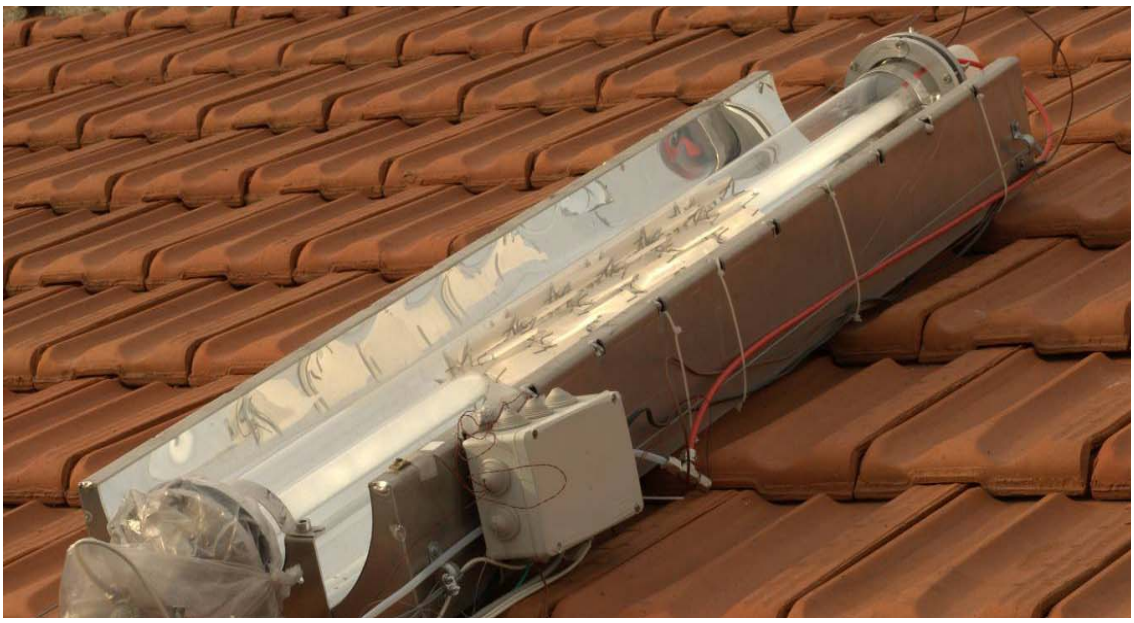

Figure 3. Photoreactor containing the plate-shaped TiO_2-$SiMgO_x$ photocatalyst placed on a roof of the wastewater treatment plant, with SSE orientation and tilted 20º, for the treatment of the air of the plant with UVA solar and lamp irradiation.

The chemical composition of the air of the primary sludge management unit was characterized in a previous work.[36] Besides hydrogen sulfide, the main pollutants found were dimethyl disulfide, dimethyl sulfide and toluene, together with other volatile organic compounds including traces of siloxanes.

3.2.1 Artificial radiation test

The first field experiment began on April 9 and was performed during one month. Only artificial radiation was employed, provided by an internal UV-lamp, in order to explore the behavior of the photoreactor with real air without the uncertainty of the solar radiation variability.

The inlet H_2S concentration exhibited cyclic fluctuations related to the sludge disposal routines, reaching a maximum every 20 minutes and a minimum approximately 14 minutes after the maximum. Additionally, during the first days of operation day-night fluctuations were observed: concentrations below 10 ppmv were typically observed in the morning and between 40-50 ppmv during the afternoon, as depicted in Figure 4A. Although some adsorption capacity of the photocatalyst was observed in the dark, irradiation was necessary to totally eliminate the H_2S present in the air. The photocatalytic activity was maintained during almost the whole month without any traces of H_2S or SO_2. H_2S was only detected in the reactor outlet after 22 days of operation; nevertheless, the concentration was not significant except for high inlet concentration values (Figure 4B).

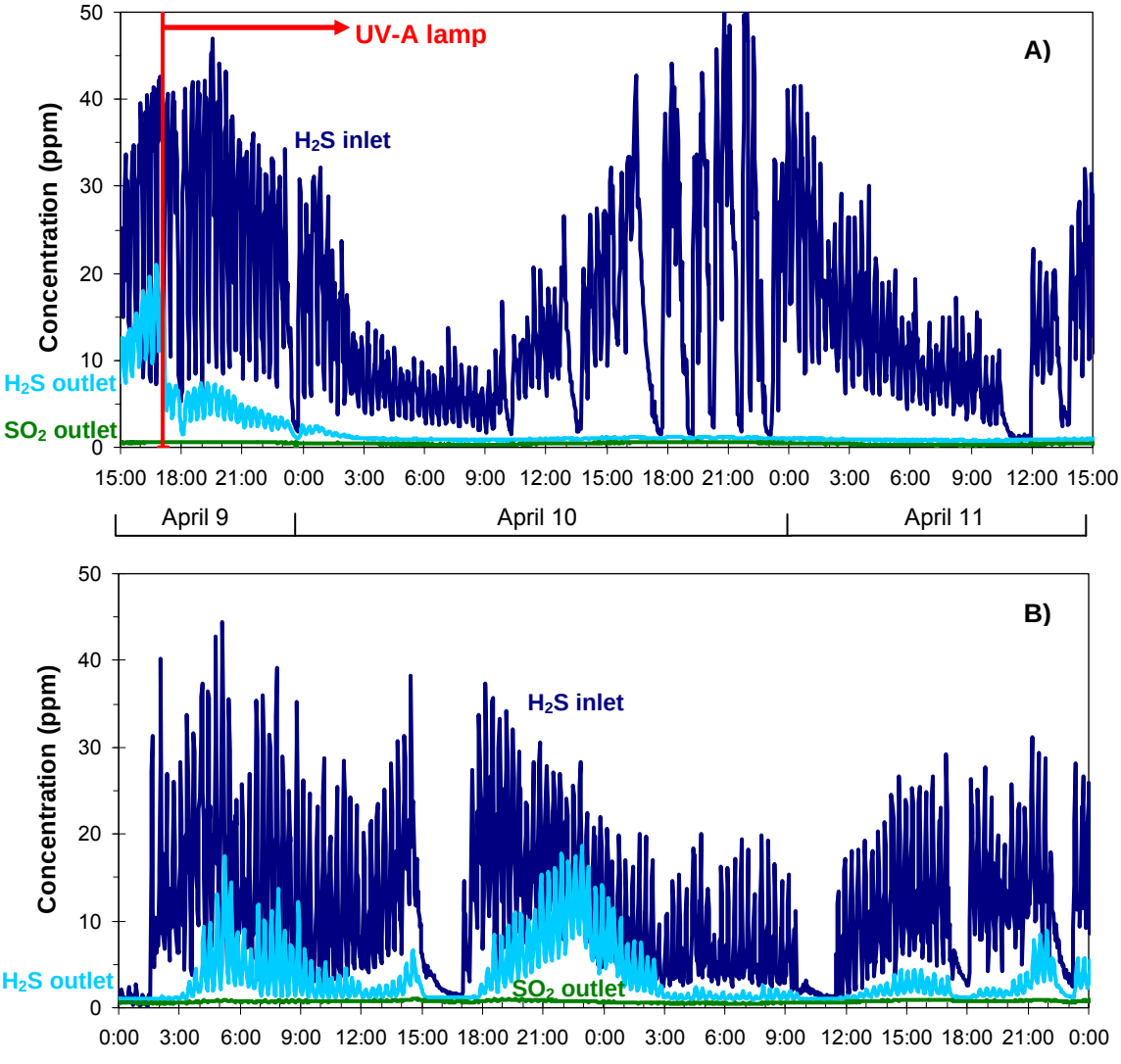

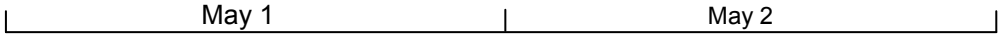

Figure 4. Photocatalytic results obtained in a WWTP (Madrid, Spain) with the internal UV-A lamp as only radiation source. Flow rate: 1L min^{-1}; photocatalyst: three structures composed by eight TiO_2-$SiMgO_x$ ceramic plates. The experiment began on April 9 (A). Deactivation started after 22 operating days (B).

3.2.2 Solar/artificial radiation test

The second experiment at the plant began on August 17. The same cyclic oscillations of the inlet concentration were observed, but day-night fluctuations were not detected. H_2S concentration values ranged the first five days between 10-40 ppmv. Then, after three days of very low values, the concentration started to progressively increase. From August 27 on, the minimum H_2S concentration was regularly above 40 ppmv, with maximum levels exceeding habitually 70 ppmv (sensor experimental detection limit).

The first ten days (August 17 to 26) the tubular photoreactor was operated with only solar radiation. During daylight hours, H_2S was completely eliminated and no traces of SO_2 were detected in the outlet stream. At night, H_2S concentration in the outlet was similar to the inlet, due to the absence of photons to activate the photocatalytic reaction. Since the distribution of the TiO_2-$SiMgO_x$ plates inside the reactor does not favor the contact with the pollutant, the adsorption was almost negligible after the first operating days. In the morning, H_2S depletion started with the first solar rays reaching the reactor. However, due to the raising temperatures, 100% H_2S conversion was only achieved at around 4 mW cm^{-2} irradiance, whereas in the afternoon total conversion was maintained up to irradiance values of around 1 mW cm^{-2}. This hysteresis cycles, previously observed and described by the authors, are caused by the modification of the adsorption properties with the temperature.[28, 36]

The continuous operation mode began on August 26. From that moment on, the lamp was turned on at sunset and turned off at sunrise every day. In Figure 5, four consecutive operation days are represented, the first two with just sunlight and the last two with both sunlight and lamp.

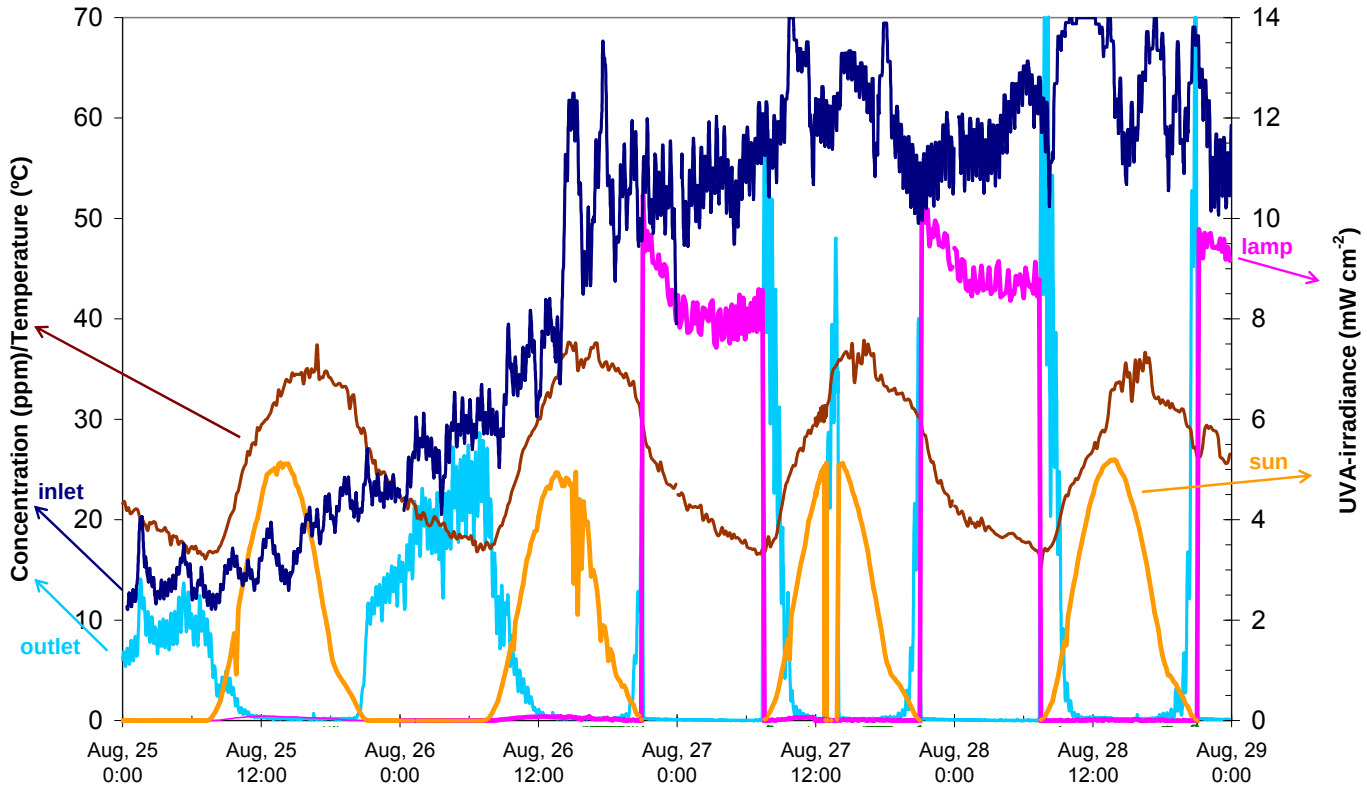

Figure 5. Photocatalytic results obtained in a WWTP (Madrid, Spain) at 1L min^{-1} flow rate with six units composed by eight TiO_2-$SiMgO_x$ ceramic plates each. The experiment began on August 17 with only solar radiation; from August 26 on, the internal lamp irradiated during the dark hours.

It was observed that the lamp had to be turned on when solar UV-A irradiance was below 2 mW cm^{-2} to avoid any presence of H_2S. Accordingly, the sensibility of the switch system was adjusted and, from that moment on, H_2S was not detected in the outlet.

The first deactivation signs appeared on September 7, as shown in Figure 6. The good adjustment of the lamp switching system can be appreciated during the morning: only few ppmv of H_2S were measured at sunrise or during the cloudy periods. In the latter day, the aforementioned differences between morning and afternoon are clearly shown.

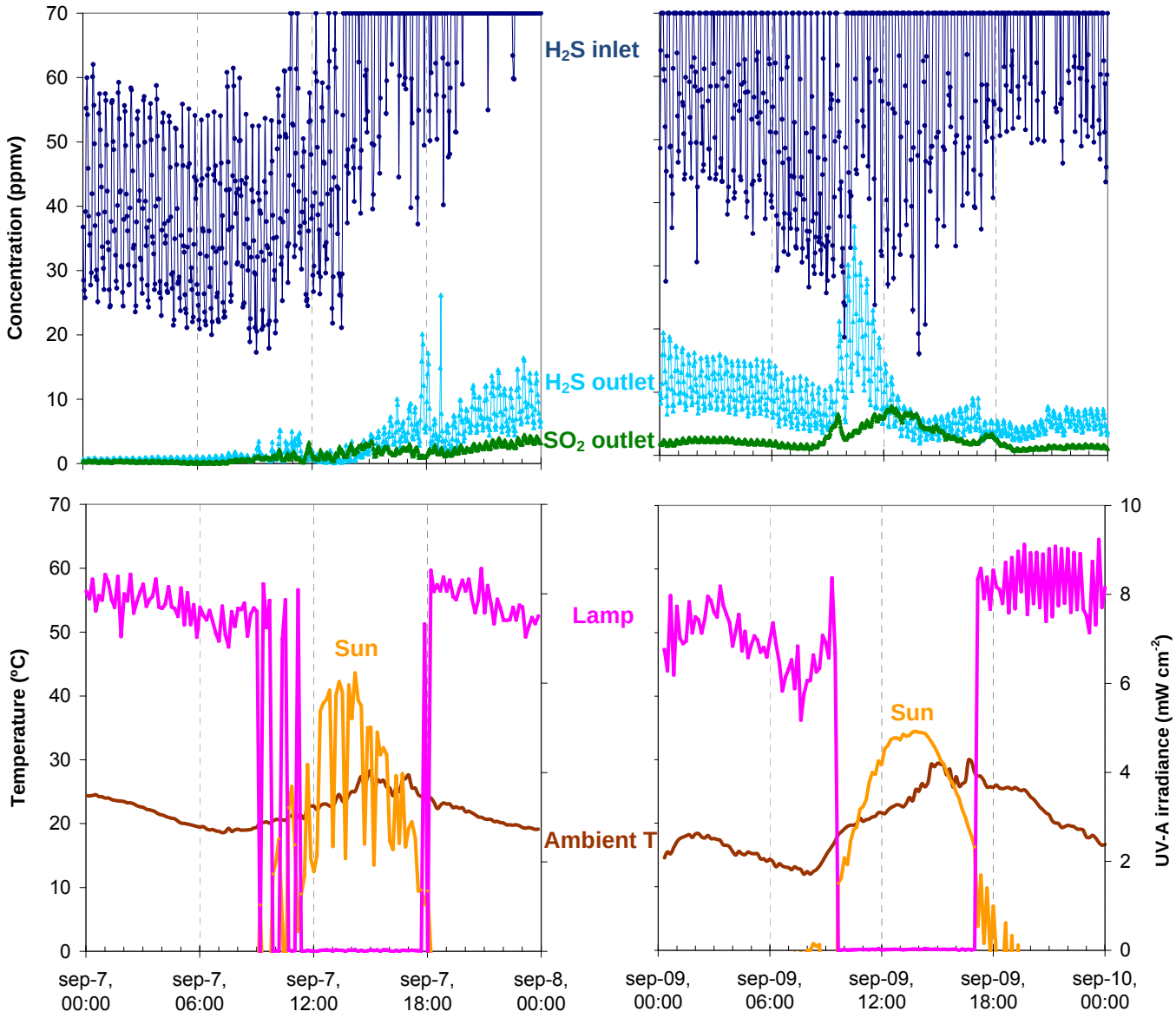

Figure 6. Photocatalytic activity on September 7 (left) and September 9 (right) in the WWTP after 22 operating days. Composition of reactor inlet and outlet (top); ambient temperature and irradiance (bottom).

In most countries, the Threshold Limit Value - Short-Term Exposure Limit (TLV-STEL) for H_2S and SO_2 is 15 ppmv and 5 ppmv, respectively, and the Time-Weighted Average (TLV-TWA) 10 and 5 ppmv, respectively.[37] Despite the considerably high H_2S inlet concentration measured in the WWTP, which probably prompted the appearance of both H_2S and SO_2 in the outlet, the TLVs were only occasionally overpassed, since an acceptable high efficiency was still maintained until the completion of the experiment (September 14).

In order to investigate the origin of the deactivation, the differences between the fresh and used materials have been studied. TG-MS analyses of the fresh and used TiO_2-$SiMgO_x$ samples are shown in Figure 7 and Figure 8. The fresh sample shows two weigh losses, apart from the loss of adsorbed water below 100ºC, one of CO_2 at 639 ºC, related to the presence of carbonates, and another one at 808ºC, related to sulfur compounds from the commercial TiO_2 used for the preparation of TiO_2-$SiMgO_x$, which contains ca. 0.6 w/w% SO_3.

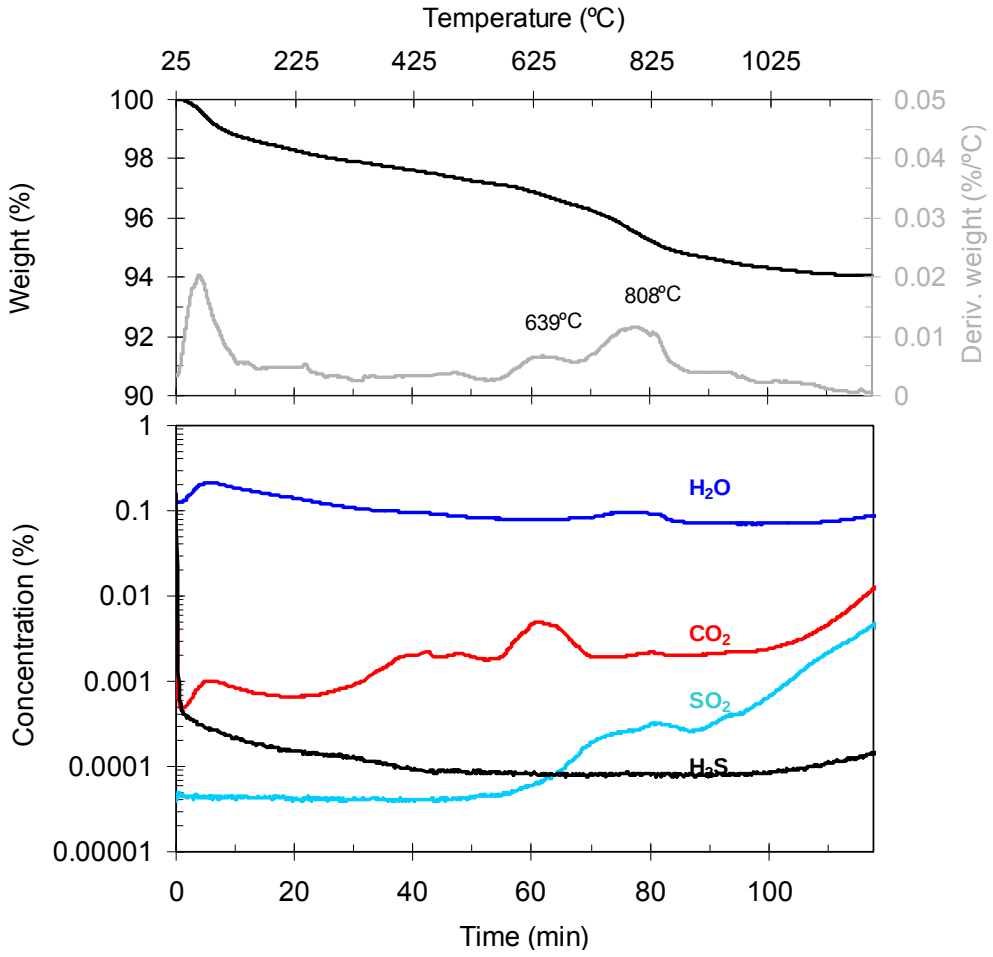

Figure 7. TG-MS results obtained with the fresh TiO_2-$SiMgO_x$ photocatalyst.

In the used sample (Figure 8), two new weight losses related to sulfur compounds were detected, at 279ºC and 479ºC, indicating the accumulation during the photocatalytic reaction of new sulfur species on the surface.

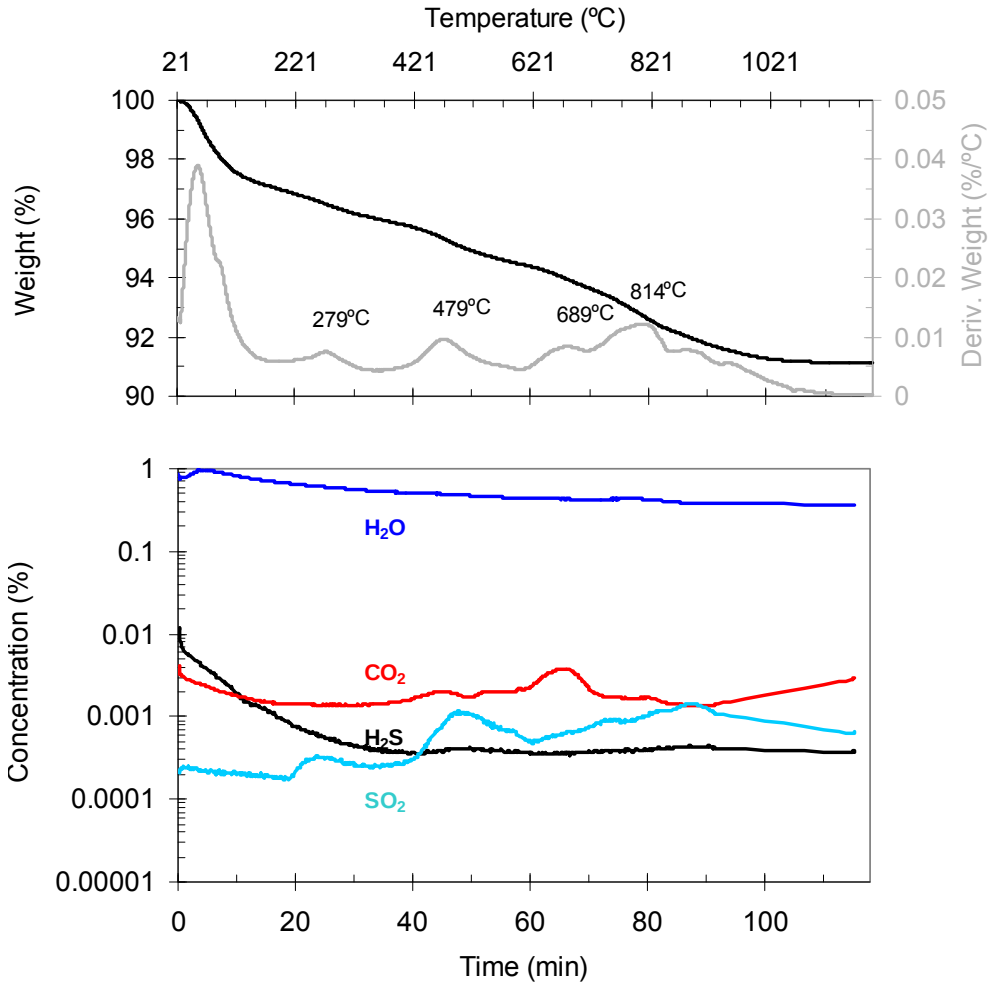

Figure 8. TG-MS results obtained with the TiO_2-$SiMgO_x$ photocatalyst after 28 operating days in the WWTP.

DRIFT spectra of the fresh and used hybrid photocatalysts were also registered (Figure 9). Since the catalyst consists of an extruded homogeneous ceramic mixture, besides the signals from physisorbed H_2O, bands from zeolitic water in the $SiMgO_x$ additive appear also in the OH region of the spectra (Figure 9, inset). These features are well known [34] and consequently their discussion has been omitted in the present study. In addition, the bending mode of OH groups from bounded water, at around 1620 cm^{-1}, is detected before and after use. In the low wavenumber region, below 1250 cm^{-1}, fingerprint signals due to the bulk TiO_2, as well as to the Si, Mg and Al oxides from the $SiMgO_x$ matrix, can be observed. For clarity reasons, in the spectrum of the used catalyst the contribution of the fresh sample has been removed by subtraction. Thus, the bands appearing in the spectrum correspond exclusively to species formed during the photocatalytic reaction.

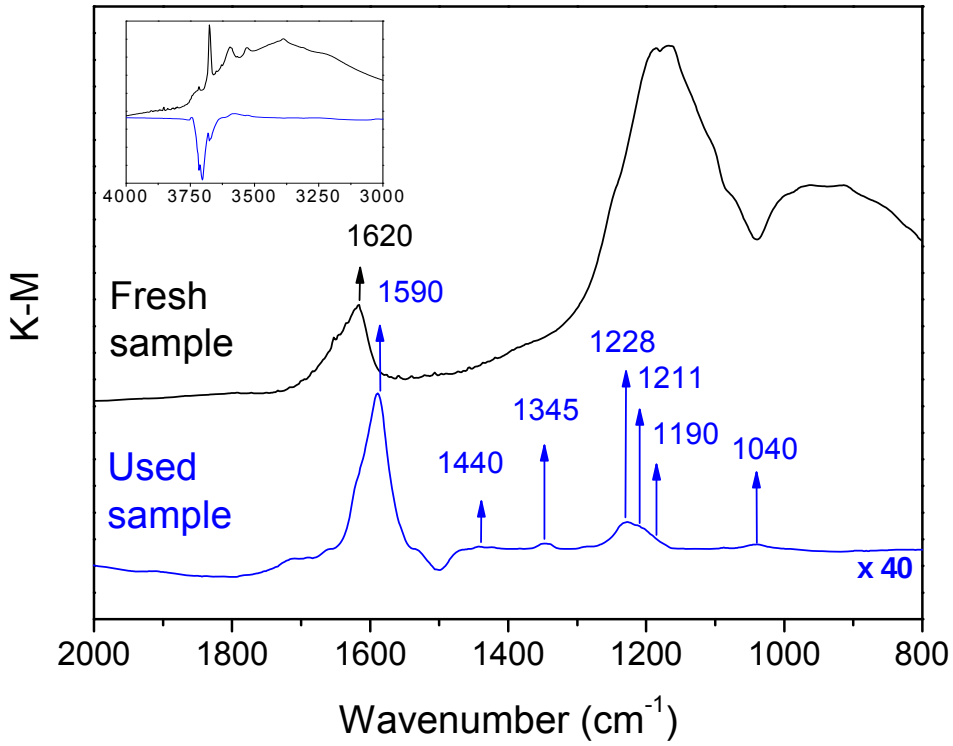

Figure 9. DRIFT spectra of the TiO_2-$SiMgO_x$ sample before and after use at the WWTP. In the latter, the contribution of the fresh photocatalyst has been removed and the intensity has been amplified for clarity reasons. The 4000-3000 cm^{-1} region of the spectra is shown in the inset.

It is worth remarking the negative features that appear in the 3750-3600 cm^{-1} region (Figure 8, inset), which suggest the active role of the hydroxyl groups during the adsorption and photocatalytic reaction. The intense band centered at 1590 cm^{-1}, along with the weak band at ca. 1440 cm^{-1}, are attributed to carboxylate species [38] formed in the photo-oxidation of the volatile organic compounds (VOCs) present in the air of the wastewater treatment plant, which have been previously identified by the authors.[36] The rest of the bands appearing in the 1400-1000 cm^{-1} interval correspond to different sulfur-containing species formed during the photo-oxidation of H_2S, and maybe of small amounts of organic sulfides also present in the air, whose unequivocal assignation is not trivial due to overlapping. Tentatively, the bands at 1211 and 1040 cm^{-1} can be assigned to SO_4^{2-} species strongly adsorbed on TiO_2 as chelating bidentate ligands. The features at 1228 and 1190 cm^{-1} are probably due to the presence of sulphite (SO_3^{2-}), while the small band that can be envisaged around 1345 cm^{-1} could be attributed to adsorbed SO_2. [39]

XPS results (data not shown) reveal an increment of C content from 2.2% to 5.8%, and, in agreement with the TG-MS and DRIFTs findings and previous H_2S photocatalytic degradation laboratory tests with TiO_2, [24] the incorporation of 0.4% S to the used photocatalyst surface due to the formation of sulfate. Additionally, a similar modification of the surface area to that observed after the laboratory tests can be appreciated in Table 1 (sample named WWTP) and no significant changes in the crystallinity have been observed in XRD analyses (data not shown). The contribution of SiO_2 deposits formed during siloxanes photo-oxidation to the deactivation, as reported for other real air tests,[40] cannot be ruled out, but the accumulation of S-containing species is probably much more

significant, due to the higher concentration of sulfur species. The fact that the adsorbent employed was based on silicates complicates the detection of possible new small contributions of Si-containing species on the surface by DRIFTs or XPS analyses.

As a conclusion, the combination TiO_2 with of an adsorbent support and an adequate reactor design allowed the use of a solar reactor prototype for the elimination of challenging sulfur compounds from the air of a wastewater treatment plant. The continuous operation mode was achieved with the help of a complementary artificial radiation source activated by an automatic switching system. The success of the photocatalytic prototype in the continuous removal of variable concentrations of H_2S was demonstrated under real conditions during one month without release of SO_2, due to the unique properties of TiO_2-$SiMgO_x$ hybrid photocatalyst.

4 ACKNOWLEDGMENTS

The authors would like to acknowledge Comunidad de Madrid (DETOX-H_2S S-0505/AMB/0406), Ministerio de Ciencia e Innovación (CTM2008-06876-C02-01/02) and AECID for financial support and M.L. Rojas-Cervantes for the TG-MS instrument.

5 SUPPORTING INFORMATION AVAILABLE

The photocatalytic experimental set-up for the laboratory tests and the porosity of TiO_2-$MgSiO_x$ samples are shown in figures included in the supporting information. This information is available free of charge via the Internet at http://pubs.acs.org/ .

6 REFERENCES

1. Lasa, H. d.; Serrano, B.; Salaices, M., *Photocatalytic Reaction Engineering*. Springer: New York, 2005.
2. Blake, D. M. *Bibliography of Work on the Photocatalytic Removal of Harzadous Compounds from Water and Air and Updates number 1, 2, 3 and 4*; National Renewable Energy Lab. Golden, CO (United States): 1994, 1995, 1996, 1999 and 2001.
3. Read, H. W.; Fu, X.; Clark, L. A.; Anderson, M. A.; Jarosch, T., Field trials of a TiO2 pellet-based photocatalytic reactor for off-gas treatment at a Soil Vapor Extraction well. *Soil and Sediment Contamination* **1996,** *5*, (2), 187-202.
4. Pichat, P.; Disdier, J.; Hoang-Van, C.; Mas, D.; Goutailler, G.; Gaysse, C., Purification / deodorization of indoor air and gaseous effluents by TiO2 photocatalysis. *Catal. Today* **2000,** *63*, 363-369.
5. Watt, A.; Magrini, K.; Carlson, L. E.; Wolfrum, E. J.; Larson, S. A.; Roth, C.; Glatzmaier, G. C., Pilot-scale demonstration of an innovative treatment for vapor emissions. *J.Air Waste Manage.Assoc.* **1999,** *49*, 1368-1373.
6. Ching, W. H.; Leung, M.; Leung, D. Y. C., Solar photocatalytic degradation of gaseous formaldehyde by sol-gel TiO2 thin film for enhancement of indoor air quality. *Solar Energy* **2004,** *77*, (2), 129-135.
7. Coronado, J. M.; Sánchez, B.; Fresno, F.; Suárez, S.; Portela, R., Influence of Catalysts Properties and Reactor Configuration on the Photocatalytic Degradation of Trichloroethylene under Sunlight Irradiation. *J.Solar Energy Eng.* **2008,** *130*, (4), 041012 (5 pages)
8. Irandoust, S.; Andersson, B., Monolithic catalysts for nonautomobile applications. *Catal. Rev. - Sci. Eng.* **1988,** *30*, (3), 341-392.
9. Blanco, J.; Avila, P.; Bahamonde, A.; Alvarez, E.; Sánchez, B.; Romero, M., Photocatalytic destruction of toluene and xylene at gas phase on a titania based monolithic catalyst. *Catal. Today* **1996,** *29*, 437-442.
10. Hossain, M. M.; Raupp, G. B.; Tempe, A.; Hay, S. O.; Obee, T. N., Three-dimensional developing flow model for photocatalytic monolith reactors. *AIChE J.* **1999,** *45:6*, 1309-1321.
11. Suzuki, K., Photocatalytic air purification on TiO2 coated honeycomb support. In *Photocatalytic Purification and Treatment of Water and Air*, D.F.Ollis; H.Al-Ekabi, Eds. Elsevier Science Publishers B.V.: 1993; pp 421-434.

12. Bhattacharyya, A.; Kawi, S.; Ray, M. B., Photocatalytic degradation of orange II by TiO2 catalysts supported on adsorbents. *Catal. Today* **2004,** *98*, (3), 431-439.
13. Kibanova, D.; Cervini-Silva, J.; Destaillats, H., Efficiency of clay - TiO2 nanocomposites on the photocatalytic elimination of a model hydrophobic air pollutant. *Environ. Sci. Technol.* **2009,** *43*, (5), 1500-1506.
14. Hossain, M.; Raupp, G. B., Polychromatic radiation field model for a honeycomb monolith photocatalytic reactor. *Chem. Eng. Sci.* **1999,** *54*, (15-16), 3027-3034.
15. Raupp, G. B.; Alexiadis, A.; Hossain, M. M.; Changrani, R., First-principles modeling, scaling laws and design of structured photocatalytic oxidation reactors for air purification. *Catal. Today* **2001,** *69*, (1-4), 41-49.
16. Carneiro, J. T.; Berger, R.; Moulijn, J. A.; Mul, G., An internally illuminated monolith reactor: Pros and cons relative to a slurry reactor. *Catal. Today* **2009,** *147*, (Supplement 1), S324-S329.
17. Hernández-Alonso, M. D.; Tejedor-Tejedor, I.; Coronado, J. M.; Anderson, M. A., Operando FTIR study of the photocatalytic oxidation of methylcyclohexane and toluene in air over TiO2–ZrO2 thin films: Influence of the aromaticity of the target molecule on deactivation. *Appl. Catal. B* **2011,** *101*, (3-4), 283-293.
18. Shiraishi, F.; Yamaguchi, S.; Ohbuchi, Y., A rapid treatment of formaldehyde in a highly tight room using a photocatalytic reactor combined with a continuous adsorption and desorption apparatus. *Chem. Eng. Sci.* **2003,** *58*, (3-6), 929-934.
19. Jo, W.-K.; Yang, C.-H., Feasibility of a tandem photocatalytic oxidation-adsorption system for removal of monoaromatic compounds at concentrations in the sub-ppm-range. *Chemosphere* **2009,** *77*, (2), 236-241.
20. Sheng, Y.; Chen, F.; Wang, X.; Sheng, G.; Fu, J., Odorous Volatile Organic Sulfides in Wastewater Treatment Plants in Guangzhou, China. *Water Environ. Res.* **2008,** *80*, (4), 324-330.
21. Canela, M. C.; Alberici, R. M.; Jardim, W. F., Gas-phase destruction of H2S using TiO2/UV-VIS. *J. Photochem. Photobiol. A* **1998,** *112*, 73-80.
22. Canela, M. C.; Alberici, R. M.; Sofía, R. C. R.; Eberlin, M. N.; Jardim, W. F., Destruction of malodorous compounds using heterogeneous photocatalysis. *Environ.Sci.Technol.* **1999,** *33*, 2788-2792.
23. Demeestere, K.; Dewulf, J.; Van Langenhove, H., Heterogeneous photocatalysis as an advanced oxidation process for the abatement of chlorinated, monocyclic aromatic and sulfurous volatile organic compounds in air: State of the art. *Crit. Rev. Environ. Sci. Technol.* **2007,** *37*, (6), 489-538.
24. Portela, R.; Sanchez, B.; Coronado, J. M.; Candal, R.; Suarez, S., Selection of TiO2-support: UV-transparent alternatives and long-term use limitations for H2S removal. *Catal. Today* **2007,** *129*, (1-2), 223-230.
25. Vorontsov, A. V.; Savinov, E. N.; Lion, C.; Smirniotis, P. G., TiO2 reactivation in photocatalytic destruction of gaseous diethyl sulfide in a coil reactor. *Appl. Catal. B* **2003,** *44*, (1), 25-40.
26. Suárez, S.; Coronado, J. M.; Portela, R.; Martín, J. C.; Yates, M.; Ávila, P.; Sánchez, B., On the preparation of TiO2-sepiolite hybrid materials for the photocatalytic degradation of TCE: influence of TiO2 distribution in the mineralization. *Environ. Sci. Technol.* **2008,** *42*, (16), 5892-5896.
27. Hewer, T. L. R.; Suárez, S.; Coronado, J. M.; Portela, R.; Avila, P.; Sanchez, B., Hybrid photocatalysts for the degradation of trichloroethylene in air. *Catal. Today* **2009,** *13*, (3-4), 302-308
28. Suárez, S.; Hewer, T. L. R.; Portela, R.; Hernandez-Alonso, M. D.; Freire, R. S.; Sanchez, B., Behaviour of TiO2-SiMgOx hybrid composites on the solar photocatalytic degradation of polluted air. *Appl. Catal. B* **2011,** *101*, (3-4), 176-182.
29. Rasmussen, S. B.; Portela, R.; Suárez, S.; Coronado, J. M.; Rojas-Cervantes, M. L.; Avila, P.; Sánchez, B., Hybrid TiO2/SiMgOX Composite for Combined Chemisorption and Photocatalytic Elimination of Gaseous H2S. *Ind. Eng. Chem. Res.* **2010,** *49*, (15), 6685–6690.
30. Portela, R.; Suárez, S.; Rasmussen, S. B.; Arconada, N.; Castro, Y.; Durán, A.; Ávila, P.; Coronado, J. M.; Sánchez, B., Photocatalytic-based strategies for H2S elimination. *Catal. Today* **2010,** *151*, (1-2), 64-70.
31. Sánchez, B.; Portela, R.; Suárez, S.; Coronado, J. M. Fotorreactor tubular para fotocatalizadores soportados (Tubular photoreactor for supported photocatalysts). PCT/ES2010/070799. PCT/ES2010/070799, 2009.
32. Rasmussen, S. B.; Due-Hansen, J.; Villarroel, M.; Gil-Llambias, F. J.; Fehrmann, R.; Ávila, P., Multidisciplinary determination of the phase distribution for VOX–ZrO2–SO42−–sepiolite catalysts for NH3-SCR. *Catal. Today* **2011,** *172*, (1), 73-77.
33. Portela, R. Eliminación fotocatalítica de H_2S en aire mediante TiO_2 soportado sobre sustratos transparentes en el UV-A. PhD thesis, Univesridad de Santiago de Compostela, 2008.
34. Jung, S. M.; Grange, P., Characterization of the surface hydroxyl properties of sepiolite and Ti(OH)4 and investigation of new properties generated over physical mixture of Ti(OH)4-sepiolite. *Appl. Surf. Sci.* **2004,** *221*, (1-4), 167-177.
35. Datta, A.; Cavell, R. G.; Tower, R. W.; George, Z. M., Claus catalysis. 1. Adsorption of SO2 on the alumina catalyst studied by FTIR and EPR spectroscopy. *J. Phys. Chem.* **1985,** *89*, (3), 443-449.
36. Portela, R.; Suárez, S.; Tessinari, R. F.; Hernández-Alonso, M. D.; Canela, M. C.; Sánchez, B., Solar/lamp-irradiated tubular photoreactor for air treatment with transparent supported photocatalysts. *Appl. Catal. B* **2011,** *105*, 95–102.

37. INSHT, *Documento sobre límites de exposición profesional para agentes químicos en España 2009*. 2009; p 156.
38. Davydov, A. A.; Rochester, C. H., *Infrared spectroscopy of adsorbed species on the surface of transition metal oxides*. John Wiley & Sons: West Sussex 1990.
39. Kataoka, S.; Lee, E.; Tejedor-Tejedor, M. I.; Anderson, M. A., Photocatalytic degradation of hydrogen sulfide and in situ FT-IR analysis of reaction products on surface of TiO2. *Appl. Catal. B* **2005,** *61*, (1-2), 159-163.
40. Hay, S. O.; Obee, T. N.; Thibaud-Erkey, C., The deactivation of photocatalytic based air purifiers by ambient siloxane. *Appl. Catal. B-Environ.* **2010,** *99*, (3-4), 435-441.